Protein Engineering, Design & Selection, 2017, vol. 30 no. 2, pp. 119–127
doi: 10.1093/protein/gzw072
Advance Access Publication Date: 22 December 2016
Original Article

Original Article

Directed evolution of P450cin for mediated electron transfer

Ketaki D. Belsare[1,5], Thomas Horn[1], Anna Joëlle Ruff[1], Ronny Martinez[1,4], Anders Magnusson[3,6], Dirk Holtmann[3], Jens Schrader[3], and Ulrich Schwaneberg[1,2,*]

[1]Lehrstuhl für Biotechnologie, RWTH Aachen University, Worringerweg 3, 52074 Aachen, Germany, [2]DWI—Leibniz-Institut für Interaktive Materialien e. V., Forckenbeckstraße 50, 52074 Aachen, Germany, and [3]Biochemical Engineering Group, DECHEMA Research Institute, Theodor-Heuss-Allee 25, 60486 Frankfurt am Main, Germany

[4]Present address: Department of Food Engineering, Universidad de La Serena, Av. Raúl Bitrán 1305, 1700000 La Serena, Chile

[5]Present address: Department of Chemistry, University of Chicago, 5735 S. Ellis Ave., SCL 317, 60637 Chicago, USA

[6]Present address: Lehrstuhl für Organic Chemistry, TU Darmstadt, Alarich-Weiss-Str. 4, 64287 Darmstadt, Germany

[*]To whom correspondence should be adressed. E-mail: u.schwaneberg@biotec.rwth-aachen.de

Edited by Dr Dick Janssen

Received 25 May 2016; Revised 28 November 2016; Editorial Decision 5 December 2016; Accepted 5 December 2016

Abstract

Directed evolution is a powerful method to optimize enzyme properties for application demands. Interesting targets are P450 monooxygenases which catalyze the stereo- and regiospecific hydroxylation of chemically inert C–H bonds. Synthesis employing P450s under cell-free reaction conditions is limited by low total turnover numbers, enzyme instability, low product yields and the requirement of the expensive co-factor NADPH. Bioelectrocatalysis is an alternative to replace NADPH in cell-free P450-catalyzed reactions. However, natural enzymes are often not suitable for using non-natural electron delivery systems. Here we report the directed evolution of a previously engineered P450 CinA-10aa-CinC fusion protein (named P450cin-ADD-CinC) to use zinc/cobalt(III) sepulchrate as electron delivery system for an increased hydroxylation activity of 1,8-cineole. Two rounds of Sequence Saturation Mutagenesis (SeSaM) each followed by one round of multiple site-saturation mutagenesis of the P450 CinA-10aa-CinC fusion protein generated a variant (Gln385His, Val386Ser, Thr77Asn, Leu88Arg; named KB8) with a 3.8-fold increase in catalytic efficiency (28 μM^{-1} min^{-1}) compared to P450cin-ADD-CinC (7 μM^{-1} min^{-1}). Furthermore, variant KB8 exhibited a 1.5-fold higher product formation (500 μM μM^{-1} P450) compared to the equimolar mixture of CinA, CinC and Fpr using NADPH as co-factor (315 μM μM^{-1} P450). In addition, electrochemical experiments with the electron delivery system platinum/cobalt(III)sepulchrate showed that the KB8 variant had a 4-fold higher product formation rate (0.16 nmol (nmol) $P450^{-1}$ min^{-1} cm^{-2}) than the P450cin-ADD-CinC (0.04 nmol (nmol) $P450^{-1}$ min^{-1} cm^{-2}). In summary, the current work shows prospects of using directed evolution to generate P450 enzymes suitable for use with alternative electron delivery systems.

Key words: bioelectrocatalysis, directed Evolution, electron mediator, P450cin, protein engineering

Introduction

The catalytic ability of P450 monooxygenases (P450s) to insert molecular oxygen chemoselectively into inert C–H bonds makes them attractive catalysts for various synthetic applications (Bernhardt, 2006; Fasan, 2012; Urlacher and Girhard, 2012). P450-catalyzed reactions are often stereo- and regioselective, and can be performed in water, at room temperature, and under atmospheric pressure. The latter is often challenging with regular chemical catalysts (Cryle *et al.*, 2003; Whitehouse *et al.*, 2012). Despite these advantages, the potential of P450s in biocatalysis particularly in cell-free catalytic systems is widely unexplored due to the requirement of cost-inefficient NADPH as the commonly used electron delivery system, low enzyme stability, low turnover numbers and low product yields. Additionally, NADPH decomposes over time and is difficult to recover once oxidized (Udit *et al.*, 2004). Various strategies to overcome the challenges associated with the use of NADPH have been reported including the regeneration of NADPH (enzymatically or electrochemically) (Kochius *et al.*, 2012; Lee *et al.*, 2013; Yu *et al.*, 2016), the use of the P450 peroxide shunt pathway (Joo *et al.*, 1999; Cirino and Arnold, 2003), the use of whole-cell systems (Cornelissen *et al.*, 2013; Ringle *et al.*, 2013), and also alternative electron delivery systems have been applied (Schwaneberg *et al.*, 2000; Shumyantseva *et al.*, 2000; Shumyantseva et al., 2015; Prasad *et al.*, 2005). Zinc dust has been reported as a cost-effective source of electrons for the mediator cobalt(III)sepulchrate ($Zn/Co^{III}sep$) for P450 BM3 (from *Bacillus megaterium*) where total turnover numbers (TTNs) of up to 570 nmol substrate per nmol P450 (for a P450 BM3 mutant) have been measured (Schwaneberg *et al.*, 2000).

Another cost-effective system for *in vitro* P450 monooxygenase catalysis involves electrochemical approaches in which an electrode acts as electron donor. Owing to the possibility to drive P450-catalyzed reactions electrochemically, P450s can be used for the development of amperometric biosensors and biosynthesis. There are generally two ways for bioelectrocatalytic reactions: (i) direct electron transfer between electrode and enzymes and (ii) indirect electron transfer using redox-active substances as electron mediators (Wong and Schwaneberg, 2003; Holtmann and Schrader, 2007; Arrocha *et al.*, 2014; Kawai *et al.*, 2014; Sugimoto *et al.*, 2015). The direct electrochemical approach involves often a surface modification of the enzyme and/or a modified electrode makes it possible to immobilize the enzyme on the surface. In contrast, the indirect electron transfer uses mediators to transfer electrons to the heme group in the active site, either directly or *via* an electron transfer component of the P450 system (Çekiç *et al.*, 2010). The electron transfer mediator may either bind in the active site of an enzyme or distal to the active site. A reported crystal structure of cytochrome P450 BM3 with the mediator $Co^{III}sep$ shows a binding site for the mediator at the entrance of the substrate access channel, distinct from binding of natural redox partner (Shehzad, 2013). Çekiç et al. (2010) reported use of platinum electrodes as electron source and $Co^{III}sep$ as electron mediator ($Pt/Co^{III}sep$) to replace NADPH in the cell-free P450cin-catalyzed hydroxylation of 1,8-cineole with a turnover number of 7 nmol $nmol^{-1}$ P450 min^{-1}. Another study shows regiospecific hydroxylation of *p*-xylene to 2,5-dimethylphenol using a P450 BM3 variant with about 10-fold lower product formation rate with $Pt/Co^{III}sep$ compared to that obtained with NADPH (Tosstorff *et al.*, 2014) implying that reactions catalyzed by indirect electron transfer from the surface of the electrode using electron mediators often suffer from low TTNs and inadequate total turnover frequencies (Udit and Gray, 2005). Nazor *et al.* (2006, 2008) reported a 6.4- and 3-fold improved P450 BM3 variants using $Zn/Co^{III}sep$ compared to the use of its natural co-factor NADPH. Our model enzyme system, P450cin catalyzes the stereoselective hydoxylation of 1,8-cineole to 2β-hydroxy-1,8-cineole. 1,8-cineole finds application in cosmetic and pharmaceutical preparations for external applications in nasal sprays, disinfectants, as analgesic and food flavoring (Rodríguez *et al.*, 2006). P450cin from *Citrobacter braakii* is a three-component class I P450 system except that its flavin-containing components resemble class II P450s (Kimmich *et al.*, 2007). The two electrons necessary for the conversion of 1,8-cineole to 2β-hydroxy-1,8-cineole are supplied by NADPH and transferred via a FAD-containing cindoxin reductase (CinB) , and an FMN-containing cindoxin (CinC) to the heme iron in the active site of P450cin (CinA). However, production of functional CinB is technically difficult and thus is replaced by *Escherichia coli* Fpr in cell-free P450cin systems. Thus, the flow of electrons in this multi-component P450cin system is from NADPH to Fpr *via* CinC to CinA. On the other hand, while using zinc dust or platinum electrodes, the flow of electrons is from platinum or zinc to CinC *via* an artificial electron transfer mediator $Co^{III}sep$ and then from CinC to CinA (Çekiç *et al.*, 2010) (Supplemental material Fig. S9).

We previously reported the construction of a functional P450 CinA-(heme center)-CinC (reductase) fusion protein separated by a linker of 10 amino acid in length, here named as P450cin-ADD-CinC, to replace the multi-component system in the hydroxylation of 1,8-cineole (Belsare *et al.*, 2014). The aim of this study was to generate, through directed evolution and semi-rational protein design, a P450cin-ADD-CinC variant able to hydroxylate 1,8-cineole to 2-β-hydroxy-1,8-cineole using the alternative electron delivery systems in which zinc dust or a platinum electrode substitute the NADPH as electron source while $Co^{III}sep$ acts as electron mediator.

Material and methods

Materials

All chemicals were of analytical grade or higher quality, and were purchased from Sigma Aldrich Chemie (Taufkrichen, Germany), AppliChem (Darmstadt, Germany) or Carl Roth (Karlsruhe, Germany) unless specified. The restriction enzymes were purchased from New England Biolabs (Frankfurt, Germany) while DNA polymerases were prepared in-house. The oligonucleotides (Supplemental material: Table S1) were purchased from Eurofins MWG Operon (Ebersberg, Germany) in salt-free form and dissolved in Milli-Q water to a concentration of 100 µM. The nucleotide analogues (dATPαS and dGTPαS) and DNA polymerases (SeSaM-Taq and 3D1) along with their respective buffers for SeSaM were obtained from the SeSaM Biotech GmbH (Aachen, Germany). All other nucleotides were purchased from Fermentas (St. Leon-Rot, Germany). The PCRs were performed in 0.2 ml thin-walled PCR tubes from Sarstedt (Nümbrecht, Germany) employing a Mastercycler Gradient PCR machine from Eppendorf (Hamburg, Germany). Plasmid DNA isolation and PCR clean up were performed using commercial kits NucleoSpin Plasmid Extraction (Macherey Nagel, Düren, Germany) and QIAquick PCR Purification Kit (Qiagen, Hilden, Germany). The platinum sheet (dimensions: 2.5 cm in length, 0.5 cm thick, 0.5 cm breadth or 2.5 cm × 0.5 cm × 0.5 cm) was purchased from Allgemeine Gold & Silber Scheide (Pforzheim, Germany). The silver–silver chloride (Ag/AgCl) electrode was purchased from Sensortechnik Meinsberg GmbH (Waldheim, Germany). The Haber luggin

capillary was purchased from Seele-Glas (Swisttal-Strassfeld, Germany). The electrochemical measurements were performed using a potentiostat from Metrohm Autolab (Riverview, Florida, USA). The DNA amount was quantified using a NanoDrop photometer from NanoDrop Technologies (Wilmington, DE, USA). DNA sequencing was performed at Eurofins MWG-Operon (Ebersberg, Germany). The analysis of obtained sequencing data was performed using Clone Manager 9 Professional Edition Software (Scientific & Educational Software, Cary, NC, USA).

Reagent and solution

Piranha solution for the cleaning of the platinum electrode surface, contained conc. H_2SO_4: 30% H_2O_2 solution (ratio 3:1). The solution was prepared on ice under a fume hood cabinet by a drop-wise addition of 30% H_2O_2 solution in concentrated H_2SO_4 including gentle swirling and was always prepared directly before usage.

Methods

Generation of random mutagenesis libraries

The Sequence Saturation Mutagenesis (SeSaM) libraries were generated as previously described (Mundhada *et al.*, 2011). The template DNA for the generation of the first SeSaM library (SeSaM I) was the previously reported P450cin-ADD-CinC (Belsare *et al.*, 2014). The template DNA for the generation of the second SeSaM library (SeSaM II) was the KB3 variant obtained after a multiple simultaneous site-saturation mutagenesis (MSSM) of the identified amino acids from SeSaM I (P450cin-ADD-CinC Gln385His, Val386Ser). For the construction of SeSaM library round I, the concentrations of dATPαS [A forward library—30%, G forward library—25%] and dGTPαS [A reverse library—30%, G reverse library—25%] were selected based on the fragmentation pattern (Supplemental material: Fig. S1). SeSaM library (50 ng each of A_rev, A_fwd, G_fwd, G_rev libraries) was cloned by PLICing as previously described (Blanusa *et al.*, 2010), and transformed in *E. coli* BL-21 Gold (DE3) $lacI^{Q1}$ cells (Inoue *et al.*, 1990).

Semi-rational evolution of P450cin-ADD-CinC

The molecular docking of Co^{III}sep into P450cin fusion protein was performed using the AutoDock algorithm embedded in the YASARA software version 13.9.8 (Krieger *et al.*, 2002), based on the crystal structure of P450cin (heme domain) reported by Meharenna *et al.* (2004) (PDB id: 1T2B). The size and location of the simulation box used for the docking experiment were chosen on the basis of a crystal structure of P450 BM3 in complex with Co^{III}sep (unpublished data) (Supplemental material: Fig. S7A, B). The crystal structure of P450cin was aligned with the crystal structure of P450 BM3 in complex with Co^{III}sep; a sequence alignment and a partial alignment of the loop region of P450 BM3 (residues 187–198 in P450 BM3 which corresponds to residues 175–179 in P450cin) were used to determine potential positions in a simulation box for subsequent docking for the Co^{III}sep. The simulation box was then built to limit the docking possibilities around this zone of the protein structure (Fig S7, C). The charge of the cobalt ion was fixed to +3 and the sepulchrate cage was placed around the cobalt ion. A total of 100 docking runs (20 runs in 5 receptor conformations) were performed and the highest ranked docking modes were selected for further analysis. Upon evaluation of the proposed docking site for Co^{III}sep, the residues Pro79, Arg80 and Tyr81 were selected as they were in close proximity from both the amino acid positions identified by random mutagenesis (Thr77 and Leu88) and in direct contact with the electron mediator Co^{III}sep. In this way, the residues Pro79, Arg80 and Tyr81 could complete a putative 'path' between Co^{III}sep and the active site.

Generation of site-saturation mutagenesis libraries

The first MSSM library was constructed at the amino acid residues Gln385 and Val386 which were identified in the first round of SeSaM. A second MSSM library was generated by simultaneous saturation at position Thr77 and Leu88 which were identified in SeSaM II. In a separate experiment, the three amino acid residues Pro79, Arg80 and Tyr81 were saturated simultaneously. The PCR protocol and primers that were used are described in the supplement (Supplementary material: Table S1). The resulting PCR product was purified using a commercial PCR purification kit following the recommended protocol and transformed into *E. coli* BL21 Gold (DE3) $lacI^{Q1}$ cells for expression (Inoue *et al.*, 1990) (see Supplementary material for a detailed protocol).

Cloning and transformation

The SeSaM libraries and the vector pALXtreme-1a were amplified individually using phosphorothioated primers (Supplemental Material, Table S1; Primer P5 and P6 for template and Primers P7 and P8 for vector backbone). Both PCRs contained: 2 U Phusion DNA polymerase, 1× Phusion DNA polymerase buffer, 0.2 mM dNTP mix, 20 µM of forward and reverse primer and 20 ng DNA template (20 ng each). The following PCR protocol was used: 98°C for 1 min (1 cycle); 20 cycles (98°C for 30 s, 65°C for 30 s and 72°C for 90 s); followed by a final extension at 72°C for 5 min (1 cycle). The amplified vector backbone was digested with *DpnI* (20 U, 37°C; 2 h), and subsequently purified for cleavage. The ligation of the vector backbone with the amplified gene was performed as previously described (Blanusa *et al.*, 2010). Subsequently, the hybridization mixture was transformed into chemically competent *E. coli* BL21 Gold (DE3) $lacI^{Q1}$ cells.

Cultivation and expression of mutant libraries

The colonies obtained for the SeSaM and MSSM libraries were transferred with sterile toothpicks into a 96-well microtiter plates (MTPs) (Greiner BioOne, Frickenhausen, Germany), pre-filled with 150 µl LB_{kan} per well (100 µg/ml kanamycin), and incubated in a microtiter plate shaker (37°C, 900 × *g*, 70% humidity; 14–16 h; Multitron II, Infors GmbH, Einsbach, Germany). Three WT and empty vector clones were included as positive and negative control in each 96-well microtiter plate. The expression cultures of SeSaM or MSSM libraries were inoculated with 6 µl from an overnight pre-culture (150 µl), and protein production was performed in 2 ml deep well plates (polypropylene plates, Brand GmbH, Wertheim, Germany) containing TB media (600 µl; supplemented with 100 µg/ml kanamycin, 0.1 mM trace element solution, 0.1 mM thiamine and 0.5 mM δ-aminolevulinic acid). The expression cultures were incubated at 37°C until an OD_{600} of 0.6 was reached. Protein production was induced with isopropyl-thio-β-galactopyranoside (IPTG; 0.1 mM final). The MTPs were incubated in a microtiter plate shaker at 27°C for 18 h (900 × *g*, 70% humidity; Multitron II, Infors GmbH, Einsbach, Germany). After cultivation the cells were harvested by centrifugation at 3200 × *g*, 4°C for 20 min, and the resulting cell pellets were frozen at −20°C.

Activity assay and gas chromatography

The 2-β-hydroxy-1,8-cineole formation in the crude cell lysate of the P450cin-ADD-CinC library was determined in 96 deep well plates using automated thin layer chromatography (TLC). The reactions contained 130 µl buffer (50 mM potassium phosphate, pH 7.4 for screening with NADPH and 50 mM potassium phosphate, 50 mM Tris–HCl, 0.25 M KCl, pH 7.4 for screening with Zn/Co^{III}sep, 30 µl crude cell lysate of the P450 CinA-ADD-CinC variants, 1,8-cineole (6 mM) and 20 µl catalase (1500 U; catalase from bovine liver, Sigma Aldrich, Taufkirchen, Germany). For the screening of the first SeSaM library all reactions were additionally supplemented with Fpr (30 µl) and initiated by the addition of NADPH (0.8 mM final concentration). For the screening of the second SeSaM library and the MSSM libraries, the reactions additionally contained the electron mediator Co^{III}sep (5 mM final concentration), and were initiated by the addition of zinc dust (5 mg in each well; Carl Roth, Karlsruhe, Germany) dispended using a solid dispenser (Resin Dispenser, Mettler-Toledo, Columbus OH, USA). The 96 deep well plates were incubated in a microtiter plate shaker for 2 h at 30°C 900 × *g* (Multitron II, Infors GmbH, Einsbach, Germany). The reaction products were extracted with 250 µl ethyl acetate containing 800 µM thymol as internal standard, dried over $MgSO_4$, and analyzed using TLC (Camag GmbH, Muttenz, Switzerland) as described in the supplement (Supplemental material: Fig. S2). 2-β-hydroxy-1,8-cineole formation using using NADPH [0.8 mM] as well as reactions using zinc dust [5 mg] and Co^{III}sep [5 mM] were performed for 2 h at 30°C using 1 µM P450 in triplicate. Reaction products were extracted with ethyl acetate and analyzed by gas chromatography–flame ionization detection (GC–FID) for determination of 2-β-hydroxy-1,8-cineole (Table 1). TTNs were obtained after a reaction time of 24 h and were calculated as µM product × μM^{-1} P450. TTNs were determined for two different concentrations of 1,8-cineole (1 and 5 mM). The reactions using platinum sheets (surface area = 2 cm^2 and Co^{III}sep [5 mM]) were performed for 6 h at 30°C using 1 µM P450 in triplicate. Reaction products were extracted with ethyl acetate and analyzed by GC–FID for determination of 2-β-hydroxy,1,8-cineole.

Gas chromatography (GC-2010, Schimadzu, Duisburg, Germany; column: 30 m × 0.25 µm × 0.25 mm, FS Supreme-5 ms from CS-Chromatographic Service, GmbH Langerwehe, Germany) was performed with the following temperature program: from 80 to 150°C with a temperature increase of 5°C/min (Injection volume: 1 µl, Split ratio: 20, carrier gas: nitrogen) by GC–FID. The retention time of 2-β-hydroxy-1,8-cineole was determined to be 9.3 min.

Table I. Product formation of the P450cin-ADD-CinC fusion protein variants (P450cin-ADD-CinC, KB1-KB8) compared to the equimolar mixture of the individual components of P450cin (CinA+CinC+Fpr)

P450cin variant	2-β-hydroxy-1,8-cineole formation [NADPH] (µM μM^{-1} P450)	2-β-hydroxy-1,8-cineole formation [Zn/Co^{III}sep] (µM μM^{-1} P450)
CinA+CinC +Fpr	315 ± 14	222 ± 3
P450cin-ADD-CinC	89 ± 2	83 ± 5
KB1	134 ± 2	110 ± 2
KB2	220 ± 4	136 ± 6
KB3	299 ± 6	203 ± 2
KB4	350 ± 4	301 ± 4
KB5	360 ± 6	306 ± 2
KB6	489 ± 2	422 ± 14
KB7	517 ± 7	491 ± 25
KB8	680 ± 6	502 ± 9
KB9	424 ± 3	408 ± 2

P450cin-ADD-CinC; KB1(Gln385His); KB2 (Val386Ser); KB3 (Gln385His, Val386Ser); KB4 (Gln385His, Val386Ser, Thr77Cys); KB5 (Gln385His, Val386Ser, Leu88Asn); KB6 (Gln385His, Val386Ser, Thr77Ser, Leu88Cys); KB7 (Gln385His, Val386Ser, Thr77Cys, Leu88Tyr); KB8 (Gln385His, Val386Ser, Thr77Asn, Leu88Arg); KB9 (Gln385His, Val386Ser, Pro79Gly, Arg80Asp, Tyr81Ser); CinA+CinC+Fpr (equimolar mix of CinA, CinC, Fpr).

Characterization of improved variants

The kinetic characterization of the WT enzyme (P450cin-ADD-CinC) and the improved variants (KB3 and KB8) for 1,8-cineole was performed in 2.2 ml Eppendorf tubes (30°C, 900 × *g*) in a total reaction volume of 1 ml. The K_M and V_{max} values were estimated by varying the concentration of 1,8-cineole from 0.05 mM to 3 mM. The reaction mixture contained: buffer (50 mM potassium phosphate, 50 mM Tris–HCl, 0.25 M KCl, pH 7.4), 0.25 µM purified enzyme, 20 µl of 1,8-cineole (final concentration: 0.05–3 mM) (Sigma Aldrich Chemie, Taufkrichen, Germany), 20 µl of catalase (1500 U; catalase from bovine liver, Sigma Aldrich, Taufkrichen, Germany), Co^{III}sep (final concentration: 5 mM) and zinc dust (5 mg). The reactions were then extracted with ethyl acetate after an interval of 5, 10, 15, 20, 30, 60 and 120 min. The final product concentrations were calculated from a standard curve obtained for 2-β-hydroxy-1,8-cineole using GC–FID. The observed data were fitted using the Michaelis–Menten equation embedded in the Origin 7.0 software (OriginLab Corporation, Northampton, MA, USA). The determination of the TTNs was performed using 1 µM purified enzyme with the same reaction conditions as for the kinetic characterization, except that the reactions were continued for 24 h (final concentration 1,8-cineole: 1 mM, and 5 mM). The product concentration of 2-β-hydroxy-1,8-cineole was determined using GC–FID.

Electrochemical characterization

The electrochemical cell for characterization consisted of platinum sheets as working electrode and counter-electrode together with Ag/AgCl as reference electrode. The working and counter electrode were dipped in reaction mixture with a total surface area of 2 cm^2. The reference electrode was inserted in a Haber-Luggin capillary tube (internal diameter 4 mm) filled with 0.5 M sodium sulfate. The electrochemical experiments were performed under potentiostatic control, and the electrochemical potential of the reaction was set to −700 mV vs Ag/AgCl. All measurements were performed in triplicate for 1, 2, 3, 4, 5 and 6 h. Thereby the reactions (final volume: 2 ml) were performed in 50 mM potassium phosphate, pH 7.4 containing 1 µM enzyme; 6 mM 1,8-cineole; 1500 U catalase, and 5 mM Co^{III}sep. The product concentration of 2-β-hydroxy-1,8-cineole was determined using GC–FID (see supplementary section for detail on the quantification using GC–FID).

Results

Evolution of P450cin-ADD-CinC

The aim of this study was the generation of a P450cin-ADD-CinC variant which is able to hydroxylate 1,8-cineole to 2-β-hydroxy-1,8-cineole using the alternative electron delivery systems Zn/Co^{III}sep and Pt/Co^{III}sep. Using directed evolution, variants showing improved activity with alternative electron delivery systems were generated.

Two rounds of SeSaM each followed by one MSSM, and in addition, a semi-rational design based on docking studies of Co^{III}sep in the P450cin crystal structure were used to reach this goal (Fig. 2). Finally, the improved P450cin variants were tested in a electrochemical approach using platinum sheets as electron source while Co^{III}Sep was used as electron mediator.

Random mutagenesis

Mutant library generation and screening

Two iterative rounds of SeSaM were performed to identify the residues which modulate the activity of P450cin towards 1,8-cineole using zinc dust as an alternative electron source and Co^{III}Sep as a electron mediator (Mundhada *et al.*, 2011). The DNA template used for construction of the SeSaM library was previously reported and is here named as P450cin-ADD-CinC (Belsare *et al.*, 2014). The quality of the generated mutant library was verified by sequencing of five randomly selected clones. The sequencing revealed 60% transitions (Ts), 20% transversions followed by transitions (TvTs; subsequent mutation), and one WT clone (Supplemental material: Table S2). The screening of the libraries was performed using an automated TLC-system as previously reported with a detection limit of 100 µM 2-β-hydroxy-1,8-cineole (Belsare *et al.*, 2014). The P450cin-ADD-CinC however, showed a product formation under the detection limit of the system (~83 µM) when Zn/Co^{III}sep was used as electron delivery system. Therefore, the first SeSaM library was screened using NADPH as electron delivery system in order to identify a variant with increased hydroxylation activity for 1,8-cineole, which could be further used in subsequent rounds of random mutagenesis for the improvement in activity towards 1,8-cineole using Zn as an alternative electron source and Co^{III}sep as electron mediator.

After screening of approximately 2700 clones, 200 clones were selected and rescreened. Following rescreening, 16 clones were selected, expressed and analyzed for product formation. Four clones showed thereby a significant increase in product formation rate compared to P450cin-ADD-CinC. DNA sequence analysis revealed that two variants KB1 (Gln385His) and KB2 (Val386Ser) each carried a single mutation.

The product formation rate of the two variants KB1 and KB2 using the alternative electron delivery system (Zn/Co^{III}sep) was 1.3- and 1.6-fold improved compared to the WT (Table 1).

Subsequently a MSSM library was generated at the positions Gln385 and Val386. According to the P450cin crystal structure both positions are deeply buried within the protein core but they are not directly interacting with the heme group (Fig. 1). The MSSM library was screened in 96 deep well plates using NADPH as electron source. The screening of ~450 clones was performed and the double mutant (Gln385His, Val386Ser) was selected as template for the construction of a second SeSaM library.

In the second round of SeSaM, 1350 clones were screened for the hydroxylation of 1,8-cineole using the alternative Zn/Co^{III}sep electron delivery system, after which 100 clones were selected for rescreening, and 16 variants were analyzed for 2-β-hydroxy-1,8-cineole formation. This resulted in the identification of variants KB4 (Gln385His, Val386Ser, Thr77Cys) and KB5 (Gln385His, Val386Ser, Leu88Asn) with a 3.5-fold improvement in product formation compared to P450cin-ADD-CinC (Table 1).

The MSSM at position Thr77 and Leu88 yielded a 5-fold improved variants KB6 (Gln385His, Val386Ser, Thr77Ser, Leu88Cys), KB7 (Gln385His, Val386Ser, Thr77Cys, Leu88Tyr) and KB8 (Gln385His, Val386Ser, Thr77Asn, Leu88Arg) (Table 1).

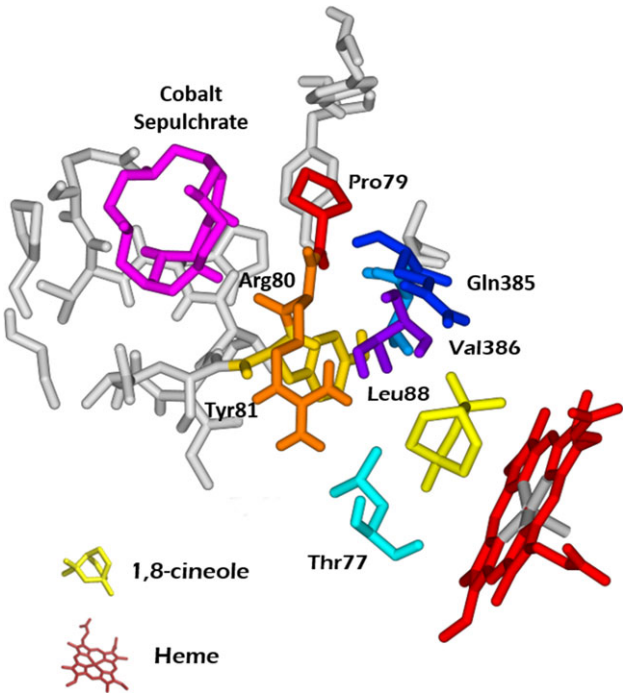

Fig. 1 Amino acid residues Gln385, Val386, Thr77 and Leu88 were identified from screening of SeSaM random mutagenesis libraries of P450cin. The positions Pro79 , Arg80 and Tyr81 were selected based on the results of docking Co^{III}sep with P450 CinA using AutoDock embedded in the YASARA software package (Version: 13.9.8.).

Comparison of hydroxylation activity for identified P450cin-ADD-CinC variants using NADPH and Zn/Co^{III}sep as electron delivery systems

In order to compare the hydroxylation activities of P450cin mutants using the artificial electron delivery system Zn/Co^{III}sep, and the natural electron delivery system with NADPH as electron source, the produced 2-β-hydroxy,1,8-cineole was quantified for P450cin-ADD-CinC, the KB8 variant, and an equimolar mixture of the individual components of the natural P450cin system (CinA+CinC+Fpr). The KB8 variant showed a 2.2-fold increased 2-β-hydroxy-1,8-cineole formation (502 ± 9 µM μM^{-1} P450) using Zn/Co^{III}sep compared to the equimolar mixture of CinA+CinC+Fpr (222 ± 3 µM μM^{-1} P450), and furthermore, the KB8 variant displayed a 1.5-fold increased product formation rate using Zn/Co^{III}sep compared to the equimolar mixture of CinA+CinC+Fpr (315 ± 13.9 µM μM^{-1} P450) using NADPH (Table 1).

Semi-rational evolution of the P450cin-ADD-CinC KB3 variant

The amino acid residues identified from the SeSaM (Gln385, Val386, Thr77, Leu88) along with the residues interacting with Co^{III}sep in the active site (Pro79, Arg80, Tyr81) of P450cin are shown in Fig. 1. The residues Pro79, Arg80 and Tyr81 are in close proximity to the Co^{III}sep, while the residues Thr77 and Leu88, which were originally found in the second round of SeSaM are predicted to interact with Co^{III}sep. Thus, the residues Pro79, Arg80 and Tyr81 were chosen for the generation of a MSSM using the KB3 variant (Gln385His, Val386Ser) as DNA template. A total of 450 clones from the resulting MSSM library were screened and

improved variant KB9 was identified and further analyzed for product formation. In order to investigate additive effects of the amino acids identified in variants KB8 and KB9, the amino acid substitutions were combined by site-directed mutagenesis. The resulting variant, however, showed no activity (data not shown).

Kinetic characterization of the WT and the two selected variants KB3 and KB8

The kinetic characterization of the WT (P450cin-ADD-CinC), and the two improved variants KB3 and KB8 was performed using the alternative electron delivery system Zn/Co^{III}sep. The kinetic parameters for the KB3 and KB8 variants in comparison to the WT are summarized in Table 2. The KB3 variant showed a 2-fold improved k_{cat} value (1.4 min^{-1}) while the KB8 variant showed a 3.7-fold increase (2.5 min^{-1}) compared to the WT (0.7 min^{-1}). Interestingly, the K_M values remained for all variants in the range of 0.09–0.1 mM suggesting similar substrate affinities for all variants (Table 2). Thus, the KB3 and KB8 variants showed a 1.8- and 3.7-fold improved k_{cat}/K_M value in comparison to the WT suggesting a better catalytic performance of these variants. In addition, the TTNs of the KB3 and KB8 variant were 3- and 6-fold increased compared to the WT (Table 2).

Electrocatalytic characterization of WT and improved variants

As alternative electron delivery system platinum electrodes were employed as electron source and Co^{III}sep as electron mediator (Pt/Co^{III}sep). The Pt/Co^{III}sep system was investigated for the variants KB1–KB9 which were identified to have an improved electrocatalytic performance using Zn/Co^{III}sep.

A maximum in 2-β-hydroxy-1,8-cineole formation was observed for the KB8 variant (61.5 ± 1.1 μM μM^{-1} P450) after 6 h reaction time. The product formation was approximately 3-fold higher than for P450cin-ADD-CinC (23.5 ± 2.5 μM μM^{-1} P450) (Table 3). The rate of product formation for the KB8 variant (0.16 nmol (nmol) P450^{-1} min^{-1} cm^{-2}) was therefore also 3-fold higher than for P450cin-ADD-CinC (0.038 nmol (nmol) P450^{-1} min^{-1} cm^{-2}).

Discussion

P450s catalyze the regio- and stereospecific oxidation of chemically inert C–H-bonds in various substrates which makes them interesting candidates for organic synthesis (Whitehouse *et al.*, 2012). In cell-free P450 systems, using alternate and cost-effective artificial electron system is one of the choice to circumvent the expensive natural co-factor NADPH (Scheller *et al.*, 2002; Bistolas *et al.*, 2005; Suprun *et al.*, 2014). However, natural P450s are not optimized for artificial electron transfer, which often led to low product titers and TTNs.

Directed evolution is a powerful approach to generate P450 variants with an improved bioelectrocatalytical properties. Çekiç *et al.* (2010) demonstrated use of platinum electrodes to transfer electrons via the electron mediator Co^{III}sep to cindoxin (CinC), which then transfers the electrons to P450cin (CinA) to hydroxylate 1,8-cineole. In our previous study, we constructed a fusion protein of CinA and CinC (P450cin-ADD-CinC) to catalyze the same reaction using *E. coli* Fpr and NADPH as electron delivery system (Belsare *et al.*, 2014).

In this work, we applied directed evolution campaign to evolve the fusion protein (P450cin-ADD-CinC) for two alternative electron transfer systems zinc/cobalt^{III}sepulchrate and platinum/cobalt^{III}sepulchrate. Zinc dust and the surface of the platinum electrode served as source of electrons, whereas cobalt^{III}sepulchrate worked as mediator.

Two rounds of SeSaM each followed by one round of MSSM at the beneficial positions generated KB8 variant (Gln385His, Val386Ser, Thr77Asn, Leu88Arg) with a 2.3- (NADPH) and 2.2-fold (Zn/Co^{III}sep) increased product formation compared to the equimolar mix of CinA+CinC+Fpr. The KB8 variant showed a slightly higher k_{cat}/K_M value of 28 min^{-1} μM^{-1} with Zn/Co^{III}sep (Table 2) compared to a (k_{cat}/K_M) of 21 min^{-1} μM^{-1} using a ratio of 1:1:1 (CinA:Fpr:CinC) and NADPH as electron delivery system (Hawkes *et al.*, 2002, 2010). Consequently, in our system, the KB8 variant in combination with Zn/Co^{III}sep can efficiently replace the multi-component P450cin system CinA/CinC/Fpr (Hawkes *et al.*, 2002, 2010). In addition, the KB8 variant was able to hydroxylate 1,8-cineole using Pt/Co^{III}sep as electron delivery system showing its applicability in bioelectrocatalysis.

The first round of SeSaM identified the exchanges of histidine at position Gln385 and serine at position Val386 to be beneficial for P450cin using Zn/Co^{III}sep and NADPH as electron delivery system. The MSSM at both positions generated the KB3 variant (Gln385His, Val386Ser) that had a 3.4-fold increased product formation after 2 h and a 1.8-fold increased catalytic efficiency compared

Table III. Product formation of the P450cin-ADD-CinC fusion protein variants (KB1–KB9) compared to the WT using Pt/Co^{III}sep system

P450cin variant	2-β-hydroxy-1,8-cineole formation [Pt/Co^{III}sep] (μM μM^{-1} P450)
P450cin-ADD-CinC	24 ± 2
KB1	18 ± 3
KB2	20 ± 3
KB3	24 ± 4
KB4	27 ± 2
KB5	28 ± 4
KB6	24 ± 2
KB7	24 ± 4
KB8	62 ± 4
KB9	33 ± 2

Table II. The kinetic parameters (k_{cat}, K_M and k_{cat}/K_M) were obtained by a non-linear regression based on the Michaelis–Menten model using the Origin 7.0 software

P450cin variant	k_{cat} [min^{-1}]	K_M [mM]	k_{cat}/K_M [μM^{-1} min^{-1}]	TTN (24 h) [μM product μM^{-1} P450]	
				1 mM	5 mM
P450cin-ADD-CinC	0.7	0.09	7	60 ± 2	260 ± 5
KB3	1.3	0.10	13	200 ± 4	562 ± 8
KB8	2.5	0.09	28	480 ± 3	1170 ± 7

to P450cin-ADD-CinC (Table 2). Structural analysis (PDB ID: 1T2B) shows that both residues are located at the bottom of the active site of P450 CinA but are not directly interacting with the heme iron (Fig. 1). Although it is difficult to directly state the reason of their functional impact it must be noted that the substitutions Gln385His and Val386Ser decrease the van der Waals radii for both residues from 219 to 191 $Å^3$. This is a reduction by 13% which could result in an increased volume of the substrate binding pocket. An improved access of the substrate to the active site might be the result of the increased substrate binding pocket. Nevertheless, the K_M value of the KB3 variant for 1,8-cineole is only slightly affected (0.09 vs 0.1 mM) suggesting similar binding behavior (Table 2).

The second round of SeSaM identified Thr77 and Leu88 as important residues for mediated catalysis and was followed by one MSSM. Variants KB6–KB8 had an increased product formation rate, and an improved k_{cat}/K_M value using either NADPH or Zn/Co^{III}sep as electron delivery systems. Structural analysis shows that both residues are located in close proximity with the 1,8-cineole and docking studies indicate that both residues are directly interacting with Co^{III}sep to mediate the electron transfer to the heme iron (Fig. 1). The mutations Thr77Asn and Leu88Arg increase the van der Waals radii at both positions from 217 to 244 $Å^3$ which is an increase of about 11%. Together with the Gln385His and Val386Ser mutations in KB3, the KB8 variant has a 2% increased van der Waals radius at all four positions together compared to P450cin-ADD-CinC. This increase is not very dramatic and might not be the reason for the improved product formation and k_{cat}/K_M value of the KB8 variant. This is consistent with the fact that the K_M value for the KB8 variant is similar compared to the P450cin-ADD-CinC and the KB3 variant (Table 2). The amino acid exchanges in the KB6-KB8 variants at the residues Thr77 and Leu88, we see that Thr77 is mainly replaced by physicochemically similar amino acids (Cys, Ser, Asn) while the hydrophobic Leu88 is replaced by mainly polar amino acids (Cys, Tyr, Arg). It seems that especially amino acid exchange Leu88Arg, in the KB8 variant seems to boost the catalytic efficiency of the P450cin enzyme. A guanidino group contains additional pi electrons which might be beneficial for electron transfer to the heme iron for both electron delivery systems, Zn/Co^{III}Sep and NADPH. Another aspect that should be discussed here is the fact that mutations in the active site induce a change in the position of the substrate binding pocket leading to an improved catalytic activity by optimization of the active site geometry. Based from our data, either the improved electron transfer from CinC to CinA or an increased catalytic rate (k_{cat}) are feasible explanations for increased hydroxylation of 1,8-cineole. (Fig. 2)

In general, all variants (KB1–KB8) show improvement for both electron delivery systems, NADPH and Zn/Co^{III}sep, suggesting that they all have similar effects on catalytic activity. P450cin shows a high sequence identity to P450cam. Phe87 from P450cam corresponding to the Thr77 in P450cin has been shown to play a major role for the camphor access in the active site (Poulos *et al.*, 1987). Our data for substitutions at Thr77 only includes conservative amino acid exchanges (Cys, Asn, Ser). A recent study proposed the electron transfer from Co^{III}sep to the heme group of P450 BM3 follows seven preferential electron transfer (ET) pathways (Verma *et al.*, 2016). A COBALT alignment of P450cin and the P450 BM3 heme domain (NCBI, Bethesda, USA) shows none of these residues involved in ET pathway in P450 BM3 are conserved in P450cin (Supplemental material Fig. S8). Interestingly, residue Thr77 in P450cin corresponds with Lys76 from P450 BM3 found to be involved in electron transfer from Co^{III}sep to the heme group in P450 BM3 suggesting a similar role in P450cin. The other residues of P450cin (Leu88, Gln385, Val386) do not directly correspond to any of the proposed P450 BM3 residues and thus, their role in the ET pathway in P450cin remains unclear (Supplemental material, Fig. S8).

Structure-guided studies for selection of amino acid residues for mutagenesis have been extensively applied in protein engineering campaigns to improve enzymes (Jakob *et al.*, 2013; Kardashliev *et al.*, 2013).

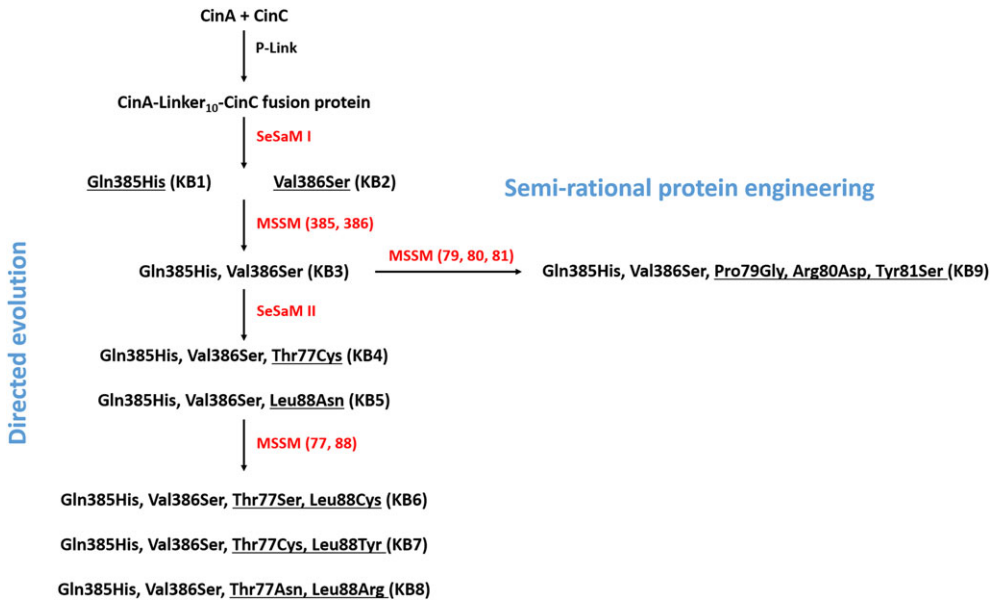

Fig. 2 Summary of the directed evolution and the semi-rational enzyme engineering for P450cin-ADD-CinC. P450cin-ADD-CinC was evolved for improvement in hydroxylation activity towards 1,8-cineole using the alternative electron delivery systems Zn/Co^{III}sep and Pt/Co^{III}sep to replace NADPH in cell-free reactions. Two iterative rounds of SeSaM was performed identifying four beneficial positions (Gln385, Val386, Thr77 and Leu88). After each round of SeSaM the beneficial positions were mutagenized using a MSSM. The semi-rational protein engineering was based on the docking studies of Co^{III}sep into the crystal structure of P450cin (PDB ID: 1T2B).

Through Co^{III}sep docking studies, we identified and simultaneously saturated residues Pro79, Arg80 and Tyr81. These positions seemed interesting and potential sites for mutagenesis as they were in very close proximity from both the amino acid positions identified by random mutagenesis (Thr77 and Leu88) and in direct contact with the electron mediator Co^{III}sep. Screening of the resulting MSSM library yielded variant KB9 (Gln385His, Val386Ser, Pro79Gly, Arg80Asp, Tyr81Ser) which showed a 1.4- and 2.0-fold increased product formation compared to the MSSM parent KB3 using both NADPH and Zn/CoIIIsep as electron delivery systems. Unfortunately, amino acid substitutions found in variants KB8 and KB9 are not compatible and further studies should address whether this incompatibility is due to stability or catalytic challenges.

The hydroxylation reaction performed using only CinA (heme) or CinC with either NADPH or zinc and Co^{III}sep, did not form 2-β-hydroxy-1,8-cineole (Supplementary information Table 4). This suggests that CinC is an essential component and required for the transfer of electrons to CinA. Direct electron transfer from Co(III) sep to CinA domain in the absence of CinC does not occur as determined by their redox potential differences (Çekiç *et al.*, 2010) which agrees with our results. Based on our experimental data and docking studies we contemplate that our docking model is not accurate but enabled us in selecting sites 79,80 and 81 for mutagenesis which yielded an improvement in variant KB9. In general, all of our mutants showed improved activity with both systems (NADPH and Co^{III}sep) as can be seen in Table 1, so we assume that directed evolution campaign and semi-rational design improved the electron transfer within the active site of P450cin and not for Co^{III}sep.

Amino acid Tyr81 in P450cin corresponds with the Asp80 of P450 BM3 that has been suggested to involved in the electron transfer from Co^{III}sep to the active site heme suggesting a similar role in P450cin (Verma *et al.*, 2016). It must be noted that multiple amino acid exchanges within the active site of enzymes are always critical since simple substitutions can deplete complex interactions such as electron transfer paths. Although putative ET paths have been analyzed with computational methods for P450cam (Tosha *et al.*, 2002; Wallrapp *et al.*, 2008) and P450 BM3 (Vidal-Limon *et al.*, 2013; Verma *et al.*, 2016), there is currently no data available for P450cin. Taken together, our results show that a combination of randomized and semi-rational enzyme design was in this case the best choice to evolve P450cin fusion protein for alternate co-factor systems and we hope that our experimental results help on further elucidating the interactions between P450cin and Co^{III}sep.

Directed evolution campaigns for P450 multi-component systems are quite challenging and often not undertaken due to the complexities with the simultanous expression of multiple enzymes, multiple rate limiting steps within the enzyme cascade, and other difficulties involved in the handling of various components in parallel. However, this study demonstrates the generation of a fully functional, catalytically improved P450 CinA-ADD-CinC fusion protein variant (KB8) for bioelectrocatalysis. The newly generated KB8 variant is suitable to replace the reconstituted P450cin system in various synthetic and electrochemical approaches, and will be a step further to use multi-component P450 systems in different bioelectrochemical applications.

Supplementary data

Supplementary data are available on *Protein Engineering, Design & Selection* online.

Acknowledgements

We thank Dr Freddi Philippart, Prof Dr J. Okuda (Chair of Organometallic Chemistry, RWTH Aachen) and Dr Markus Reichelt (Lehrstuhl für Makromolekulare Materialien und Oberflächen; DWI—Leibniz-Institut für Interaktive Materialien) for the synthesis and the NMR analysis of cobalt^{III}sepulchrate.

Conflict of interests

The authors declare no conflict of interests with this study.

Funding

The work was supported by the Arbeitsgemeinschaft industrieller Forschungsvereinigungen (AiF) Otto von Guericke e. V. [grant number: F 519F]. The project funders had no role in study design, data collection and interpretation, or the the decision to submit the work for publication.

References

Arrocha,A.A., Cano-Castillo,U., Aguila,S.A. and Vazquez-Duhalt,R. (2014) *Biosens. Bioelectron.*, **61**, 569–574.

Belsare,K.D., Ruff,A.J., Martinez,R., Shivange,A.V., Mundhada,H., Holtmann,D., Schrader,J. and Schwaneberg,U. (2014) *BioTechniques*, **57**, 13.

Bernhardt,,R. (2006) *J. Biotechnol.*, **124**, 128–145.

Bistolas,N., Wollenberger,U., Jung,C. and Scheller,F.W. (2005) *Biosens. Bioelectron.*, **20**, 2408–2423.

Blanusa,M., Schenk,A., Sadeghi,H., Marienhagen,J. and Schwaneberg,U. (2010) *Anal. Biochem.*, **406**, 141–146.

Çekiç,S.Z., Holtmann,D., Güven,G., Mangold,K.M., Schwaneberg,U. and Schrader,J. (2010) *Electrochem. Commun.*, **12**, 1547–1550.

Cirino,P. C. and Arnold,F. H. (2003) *Angew. Chem. Int. Ed. Engl.*, **115**, 3421–3423.

Cornelissen,S., Julsing,M.K., Volmer,J., Riechert,O., Schmid,A. and Bühler,B. (2013) *Biotechnol. Bioeng.*, **110**, 1282–1292.

Cryle,M.J., Stok,J.E. and De Voss,J.J. (2003) *Aust. J. Chem.*, **56**, 749–762.

Fasan,R. (2012) *ACS Catal.*, **2**, 647–666.

Hawkes,D.B., Adams,G.W., Burlingame,A.L., Ortiz de Montellano,P.R. and De Voss.,J.J. (2002) *J. Biol. Chem.*, **277**, 27725–27732.

Hawkes,D.B., Slessor,K.E., Bernhardt,P.V. and De Voss,J.J. (2010) *Chembiochem.*, **11**, 1107–1114.

Holtmann,D. and Schrader,J. (2007) *Modern Biooxidation: Enzymes, Reactions and Applications*, 265–290.

Inoue,H., Nojima,H. and Okayama,H. (1990) *Gene*, **96**, 23–28.

Jakob,F., Martinez,R., Mandawe,J., Hellmuth,H., Siegert,P., Maurer,K.H. and Schwaneberg,U. (2013) *Appl. Microbiol. Biotechnol.*, **97**, 6793–6802.

Joo,H., Lin,Z. and Arnold,F.H. (1999) *Nature*, **399**, 670–673.

Kardashliev,T., Ruff,A.J., Zhao,J. and Schwaneberg,U. (2013) *Mol. Biotechnol.*, 1–10.

Kawai,S., Yakushi,T., Matsuhita,K., Kitazumi,Y., Shirai,O. and Kano,K. (2014) *Electrochem. Commun.*, **38**, 28–31.

Kimmich,N., Das,A., Sevrioukova,I., Meharenna,Y., Sligar,S.G. and Poulos, T.L. (2007) *J. Biol. Chem.*, **282**, 27006–27011.

Kochius,S., Magnusson,A.O., Hollmann,F., Schrader,J. and Holtmann,D. (2012) *Appl. Microbiol. Biotechnol.*, **93**, 2251–2264.

Krieger,E., Koraimann,G. and Vriend,G. (2002) *Proteins Struct. Funct. Bioinf.*, **47**, 393–402.

Lee,S.H, Kwon,Y.C., Kim,D.M and Park,C.B. (2013) *Biotechnol. Bioeng.*, **2**, 383–390.

Meharenna,Y.T., Li,H., Hawkes,D.B., Pearson,A.G., De Voss,J. and Poulos, T.L. (2004) *Biochemistry*, **43**, 9487–9494.

Mundhada,H., Marienhagen,J., Scacioc,A., Schenk,A., Roccatano,D. and Schwaneberg,U. (2011) *Chembiochem*, **12**, 1595–1601.

Nazor,J. and Schwaneberg,U. (2006) *Chembiochem*, **7**, 638–644.

Nazor,J., Dannenmann,S., Adjei,R.O., Fordjour,Y.B., Ghampson,I.T., Blanusa,M., Roccatano,D. and Schwaneberg,U. (2008) *Protein Eng. Des. Sel.*, **21**, 29–35.

Poulos,T.L., Finzel,B.C. and Howard,A.J. (1987) *J. Mol. Biol.*, **195**, 687–700.

Prasad,S., Murugan,R. and Mitra,S. (2005) *Biochem. Biophys. Res. Commun.*, **335**, 590–595.

Ringle,M., Khatri,Y., Zapp,J., Hannemann,F. and Bernhardt,R. (2013) *Appl. Microbiol. Biotechnol.*, **97**, 7741–7754.

Rodríguez,P., Sierra,W., Rodríguez,S. and Menéndez,P. (2006) *Electron. J. Biotechnol.*, **9**, 232–236.

Scheller,F.W., Wollenberger,U., Lei,C., Jin,W., Ge,B., Lehmann,C., Lisdat,F. and Fridman,V. (2002) *J. Biotechnol.*, **82**, 411–424.

Schwaneberg,U., Appel,D., Schmitt,J. and Schmid,R.D. (2000) *J. Biotechnol.*, **84**, 249–257.

Shehzad,A. (2013) *Insights into the Structural Basis for Activity and Selectivity of P450 BM3Monooxygenase*. RWTH Aachen University, Germany.

Shumyantseva,V.V., Bulko,T.V., Bachmann,T.T., Bilitewski,U., Schmid,R.D. and Archakov,A.I. (2000) *Arch. Biochem. Biophys.*, **377**, 43–48.

Shumyantseva,V.V., Bulko,T., Shich,E., Makhova,A., Kuzikov,A. and Archakov,A. (2015) *Adv. Exp. Med. Biol.*, **851**, 229–246.

Sugimoto,Y., Kitazumi,Y., Tsujimura,S., Shirai,O., Yamamoto,M. and Kano,K. (2015) *Biosens. Bioelectron.*, **63**, 138–144.

Suprun,E.V., Shumyantseva,V.V. and Archakov,A.I. (2014) *Electrochim. Acta*, **140**, 72–82.

Tosha,T., Yoshioka,S., Hori,H., Takahashi,S., Ishimori,K. and Morishima,I. (2002) *Biochemistry*, **41**, 13883–13893.

Tosstorff,A., Dennig,A., Ruff,A.J., Schwaneberg,U., Sieber,V., Mangold,K.M., Schrader,J. and Holtmann,D. (2014) *J. Mol. Catal. B Enzym.*, **108**, 51–58.

Udit,A.K., Arnold,F.H. and Gray,H.B. (2004) *J. Inorg. Biochem.*, **98**, 1547–1550.

Udit,A.K. and Gray,H.B. (2005) *Biochem. Biophys. Res. Commun.*, **338**, 470–476.

Urlacher,V.B. and Girhard,M. (2012) *Trends Biotechnol.*, **30**, 26–36.

Verma,R., Schwaneberg,U., Holtmann,D. and Roccatano,D. (2016) *J. Chem. Theory Comput.*, **12**, 353–363.

Vidal-Limon,A., Aguila,S., Ayala,M., Batista,C.V. and Vazquez-Duhalt,R. (2013) *J. Inorg. Biochem.*, **122**, 18–26.

Wallrapp,F., Masone,D. and Guallar,V. (2008) *J. Phys. Chem. A*, **112**, 12989–12994.

Whitehouse,C.J., Bell,S.G. and Wong,L.L. (2012) *Chem. Soc. Rev.*, **41**, 1218–1260.

Wong,T.S. and Schwaneberg,U. (2003) *Curr. Opin. Biotechnol.*, **14**, 590–596.

Yu,T., Li,J.F., Zhu,L.J., Hu,D., Deng,C., Cai,Y.T. and Wu,M.C. (2016) *Ann. Microbiol.*, **66**, 343–350.